# Self-organized growth of microsized Ge wires on Si (111) surfaces

Zhangcheng Xu,[1,*] Yating Zhang,[1] Randall L. Headrick,[2] Hua Zhou,[2] Lan Zhou,[2] and Tomoe Fukamachi[3]
[1]*Nano-photonics Laboratory, TEDA-APS, TEDA College, Nankai University, Tianjin 300457, People's Republic of China*
[2]*Department of Physics, The University of Vermont, Burlington, Vermont 05405, USA*
[3]*Saitama Institute of Technology, 1690 Fusaiji, Fukaya, Saitama 3690293, Japan*
(Received 27 January 2007; revised manuscript received 18 April 2007; published 29 June 2007)

Microsized Ge wires can appear spontaneously when grown on a vicinal Si (111) surface miscut by 4° along the [11−2] direction by using molecular-beam epitaxy. Time-resolved *in situ* grazing incidence small-angle scattering of x rays, atomic force microscopy, and micro-Raman scattering show that the formation of Ge microwires is due to coalescence of islands along the step edges and ripening of the structures accompanied by a partial consumption of the wetting layer.

DOI: 10.1103/PhysRevB.75.233310 PACS number(s): 81.10.Aj, 68.35.Bs, 68.37.Ps, 68.55.−a

Self-organization of patterns is a common phenomenon in nature.[1] Epitaxy of Ge on Si surfaces can be regarded as a model system for nanostructure self-organization on solid surfaces.[2–4] Spontaneous formation of Ge quantum dots on singular Si surfaces and Ge quantum wires or alloy superlattices on vicinal Si surfaces has been observed and intensively studied.[5–9] However, the possibility of the formation of self-organized patterns of Ge on Si surfaces on the micrometer scale is unknown. Here, we show that Ge microwire (MWR) arrays can appear spontaneously when grown on a vicinal Si (111) surface miscut by 4° along the [11−2] direction, at a very low growth rate, with a molecular-beam epitaxy instrument.

Material growth was performed on a molecular-beam epitaxy instrument with a Ge solid source, at X21 of National Synchrotron Light Source, Brookhaven National Laboratory. The base pressure of the growth chamber is $1\times10^{-10}$ Torr. Three *p*-type Si (111) substrates were used. Two substrates (samples 1 and 2) have a miscut angle of 4° toward the [11−2] direction, whereas the third one (sample 3) has a miscut angle smaller than 0.1°, as determined by x-ray diffraction. The native surface oxide was removed with 40% $NH_4F$ solution[10] before mounting the substrate on a molybdenum plate. The $(7\times7)$ reconstructed surface was obtained by flashing the substrate at 850 °C, then the substrate was cooled down to 560 °C for growth. The substrate temperature was measured by using an infrared pyrometer.

The reflection high-energy electron-diffraction (RHEED) patterns from the surface of sample 1 before [Fig. 1(a)] and after [Fig. 1(b)] the Ge growth were taken when the incident electron beam was parallel to the [1−10] direction. Bright spots coexist with the $(7\times7)$ pattern background, indicating that the surface contains both the $(7\times7)$ terraces and the step bunches.[11] After finishing the growth, RHEED pattern shows Ge $(5\times5)$ reconstructed surface. The deposition rate of Ge was determined by using the critical thickness (2.5 bilayers, 1 BL$=1.44\times10^{15}$ atoms/cm$^2$)[4] of the wetting layer on singular Si (111) surfaces. It takes 15 min when the RHEED pattern changes from streaky to spotty, which amounts to a growth rate of 0.167 BL per minute. Therefore, the total deposition amount is 12.4 BL for sample 1 (74 min) and 15.7 BL for sample 2 (94 min).

Time-resolved *in situ* grazing incidence small-angle scattering of x rays (GISAXS) was used to monitor the growth of Ge MWRs for sample 1. Synchrotron x-ray radiation was tuned at the wavelength of 0.1124 nm. X rays impinge the surface at 0.15° (the critical angle of total reflection for Si) along the [1−10] direction. The GISAXS data were acquired by scanning a point *p-i-n* diode in a plane nearly parallel to the substrate, with a fixed exit angle of 0.85°. As the growth rate is extremely low, the surface change during fast scanning one spectrum can be negligible. After growth, atomic force microscopy (AFM), grazing incident x-ray diffraction (GIXRD), and micro-Raman spectroscopy were carried out.

AFM measurements were performed on a Nanoscope III instrument in air in the contact mode. Figure 2(a) shows that Ge nanodots were formed on the singular Si (111) surface of sample 3, which coincides with the conventional Stranski-Krastonow growth.[2–4] However, Ge MWRs were formed on the vicinal Si (111) surfaces of samples 1 and 2, as shown in Figs. 2(b) and 2(c), respectively. The Ge MWRs are well aligned along the [1−10] direction. A typical Ge MWR is 5 $\mu$m (6.5 $\mu$m) long, 800 nm (1000 nm) wide, and 40 nm (54 nm) high, for sample 1 (2). Note that the density of MWRs was decreased from $2\times10^7$/cm$^2$ for sample 1 to $4\times10^6$/cm$^2$ for sample 2 upon longer deposition time of 20 min for sample 2. The surface plot and magnification of the circled area in Fig. 2(b) are shown in Figs. 2(d) and 2(e). It can be seen that the cross section of a MWR is an asymmetric triangle shape. Cross-sectional analysis [Fig. 2(f)] shows that the inclination angle of the *AB* plane with respect to the mean surfaces is about 4° regardless of the analyzing points, indicating that the *AB* plane is parallel to

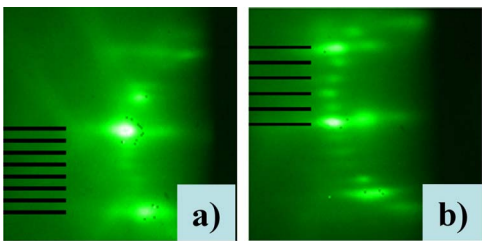


FIG. 1. (Color online) (a) The RHEED pattern of the surface before growing Ge MWRs. (b) The RHEED pattern of the surface after finishing growing Ge MWRs. The black lines are drawn to show the spacing of the diffraction lines.

 

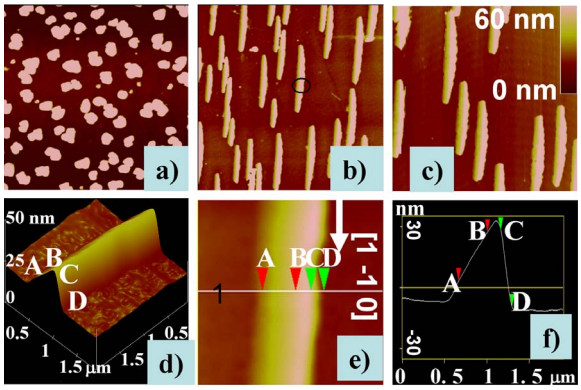


FIG. 2. (Color online) The AFM image ($15\times15$ $\mu m^2$) of (a) Ge nanodots (sample 3) and (b) Ge MWR arrays (sample 1). The $z$ scale in (a) and (b) is 40 nm. (c) Ge MWR arrays (sample 2). (d) The surface plot of the circled region of (b). (e) The magnification of the circled region of (b). (f) The line analysis along line 1 in (e).

the (111) lattice planes. However, the inclination angle of the *CD* plane depends on the analyzing points, ranging from 9° to 17°. Furthermore, undulations can be clearly seen on the right side of the wires and the MWRs have a width which is maximum in the middle of the "wire." Some isolated islands can also be seen in Figs. 1(b) and 1(c). Small holes can be identified in some of the wires. All these features suggest that the MWRs were formed due to coalescence of islands clustering at the step edges.

To determine the lateral elastic strain in the Ge MWRs, in-plane GIXRD measurements were performed on a Rigaku ATX-G x-ray diffractometer, with Cu $K\alpha_1$ x rays monochromated with double Ge (220) crystals, at the incidence angle of $\phi$=0.25°. (close to the critical angle for total reflection). As shown in Fig. 3, two peaks can be clearly resolved, one corresponding to Si (2−20) substrate, and the other to the Ge MWRs. The lateral strain can be calculated to be 1.2%, indicating elastic strain relaxation and Ge-Si intermixing, which is further supported in the micro-Raman spectroscopy.

The local phonon modes and the Ge composition within the MWRs can be determined via micro-Raman scattering spectroscopy. The measurements were performed on a micro-Raman spectroscopic system (Renishaw) with a 632.8 nm He-Ne laser as the excitation source, at room temperature, in the backscattering configuration. The focus size is about 1 $\mu$m in diameter, slightly wider than the Ge MWRs of sample 1. As shown in Fig. 4, the GeGe longitudinal-optical (LO) mode at 295 $cm^{-1}$, the SiGe LO mode at 407 $cm^{-1}$, and the second-order transverse-acoustic (2TA) phonon mode for Si at 302 $cm^{-1}$ are observed from the Ge MWR. However, no Ge-related signal is observed in the region between the Ge MWRs, indicating that the formation of the MWRs is accompanied by a partial consumption of the wetting layer. The frequency position of the GeGe optical phonons is slightly shifted to the lower frequencies with respect to that for bulk crystalline Ge (300 $cm^{-1}$). The Ge composition can be estimated to be around 80% according to Ref. 12, which means that Ge-Si intermixing occurs during growth. The intermixing can have an effect in decreasing the strain energy of MWRs, as previously found for Ge/Si quantum dots.[13]

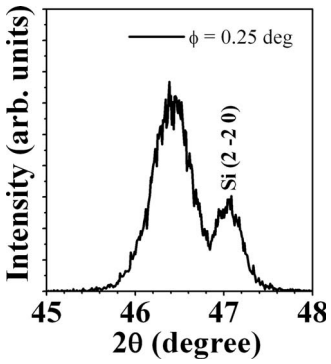


FIG. 3. The in-plane GIXRD of Ge MWRs around the Si (2−20) reflection peak.

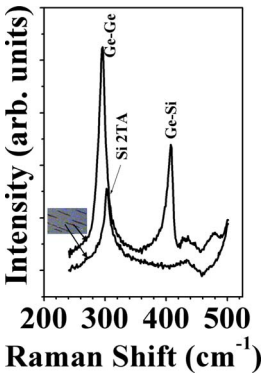


FIG. 4. (Color online) Micro-Raman spectra taken from (a) one Ge MWR and (b) the region between the Ge MWRs. The inset shows the optical microscope image of the surface.

Time-resolved *in situ* GISAXS measurements were performed for sample 1, which can trace the evolution of surface morphology during growth,[14] to understand the growth mechanism of Ge MWRs. The scattering geometry is shown in the right inset of Fig. 5(a), which is similar to that in Ref. 14, except that a point *p-i-n* detector instead of a charge coupled device was used in our experiments. Figure 5(a) shows the evolution of GISAXS spectra at different times after starting deposition. It can be seen that there is a "shoulder" (labeled as P1, at $q_y$=0.051 $nm^{-1}$, $q_y$ being the $y$ component of the scattering wave vector) on the right side of the central peak ($q_y$=0 $nm^{-1}$) of the mean surface in the GISAXS spectrum before growth. P1 represents the (111) terraces on the surface, as the angle between this facet and the mean surface is around 4° according to atan($q_y/q_z$), $q_z$ =0.7 $nm^{-1}$ being the $z$ component of the scattering wave vector, which coincides with the x-ray-diffraction determination of the miscut angle. After 15 min of growth (2.5 BL), a new broad shoulder (labeled as P2, $q_y$=−0.12 $nm^{-1}$) can be clearly seen, indicating that new facets have been formed. For the MWRs, P2 is related to facet 2 indicated in the inset of Fig. 5(b), as atan($q_y/q_z$) is around 10°. As shown in the left inset of Fig. 5(a), the spectrum at 74 min can be decomposed into three peaks of three Lorentzian functions. The peak width of P2 is nearly 1.7 times that of peak P1, reflect-

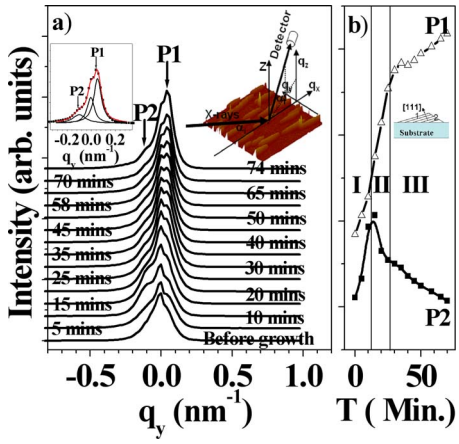


FIG. 5. (Color online) (a) Time-resolved *in situ* GISAXS spectra during growing Ge MWRs (sample 1): the right inset shows the scattering geometry, the scattering factor is defined in the same way as in Ref. 14; the left inset shows the fitting of the GISAXS spectrum after finishing the growth, with three Lorentzian functions. (b) The intensity variation of P1 and P2 as a function of time.

ing the inhomogeneous distribution of facet 2 for different wires.

Figure 5(b) shows the intensity variation of P1 and P2 as a function of growth time. It can be seen that the intensity of P1 increases in the whole time range, indicating the continuous growth of (111) lattice planes. The intensity of P2 increases first and reaches the maximum at 15 min, then decreases drastically, and finally decreases steadily. The intensity change of P2 suggests that the formation process of Ge MWRs consists of three stages, as shown in Fig. 5(b). In stage I, Ge adatoms attach along the existing surface steps or step bunches of Si surfaces, in the $[1-10]$ direction, as the intensity ratio of P1 and P2 does not change so much. Small and separated islands form at the step edges and they will have a side with (111) facets and the other side bounded by steeper orientations.[15] When the Ge deposition is continued, nearby islands will coalesce because the employed temperature renders ripening of coherent islands relatively slow.[16] The system enters stage II. As the scattering intensity is proportional to "scatter" densities,[17] the drastic decrease of P2 intensity indicates a drastic decrease of the total number of Ge islands. As the islands are aligned along the step edges, coalescence of a chain of islands will give rise to a "microwire." Coalescence is also accompanied by dislocation introduction, which will lead to ripening of the structure in stage III, as indicated in the P2 intensity decrease and the AFM observation in Fig. 2(c). Coalescence of individual islands could possibly explain the undulation observed in the MWRs.

In summary, the spontaneous formation of Ge MWR arrays on vicinal Si (111) surfaces verified that self-organization patterning on the micrometer scale during strained-layer epitaxy can be realized. The Ge MWRs are well aligned along the $[1-10]$ directions. The MWRs are typically 5 $\mu$m long, 0.8 $\mu$m wide, and 40 nm high, with an asymmetric triangular cross section. Atomic force microscopy and high resolution x-ray diffraction measurements show that one facet of the MWR is parallel to the (111) lattice planes. The Ge composition inside the MWRs is around 80% according to the micro-Raman analysis. Time-resolved *in situ* grazing incidence small-angle scattering of x rays measurement indicates that the formation of Ge MWRs is due to coalescence of islands along the step edges and ripening of the structures. This phenomenon should be useful not only for testing theories of strained-layer epitaxy[18] but also for obtaining structures with large magnetic anisotropy by incorporating some magnetic material into the Ge MWRs, which could be used in the technology of spintronics.[19]

Lin Yang, Chi-Chang Kao, Wolfgang A. Caliebe, Karl F. Ludwig, Ahmet Ozcan, Yao Cheng, Tao Jiang, Jie Zhang, R. Negishi, M. Yoshizawa, Jialing Xu, Zhanguo Wang, Jingjun Xu, Xiaoshuang Chen, Wei Lu, and Y. Horikoshi are acknowledged. This work is partly supported by the Natural Science Foundation of China (Grants No. 60444010 and No. 60506013), the U.S. Department of Energy (DE-FG-0203-ER-46032), the U.S. National Science Foundation Instrumentation for Materials Research (DMR-0216704), the SRF for ROCS (SEM), the startup fund for new employees of Nankai University, the Program for New Century Excellent Talents in Universities (NCET, China), the Advanced Science Research Laboratory of SIT, and Marubun Research Promotion Foundation. Use of the National Synchrotron Light Source, Brookhaven National Laboratory, was supported by the U.S. Department of Energy.

*Author to whom correspondence should be addressed. zcxu@nankai.edu.cn

[1] H. Haken, *Synergetics. An Introduction: Nonequilibrium Phase Transitions and Self-organization in Physics, Chemistry and Biology* (Springer, Berlin, 1983).
[2] Z. Y. Zhang and M. G. Lagally, Science **276**, 377 (1997).
[3] J. V. Barth, G. Costantini, and K. Kern, Nature (London) **437**, 671 (2005).
[4] C. Teichert, Phys. Rep. **365**, 335 (2002).
[5] A. Sgarlata, P. D. Szkutnik, A. Balzarotti, N. Motta, and F. Rosei, Appl. Phys. Lett. **83**, 4002 (2003).
[6] P. D. Szkutnik, A. Sgarlata, N. Motta, and A. Balzarotti, Mater. Sci. Eng., C **23**, 1053 (2003).
[7] G. Jin, Y. S. Tang, J. L. Liu, and K. L. Wang, Appl. Phys. Lett. **74**, 2471 (1999).
[8] K. Sumitomo, F. Lin, Y. Homma, and T. Ogino, Appl. Surf. Sci. **237**, 68 (2004).
[9] A. Ronda, M. Abdallah, J. M. Gay, J. Stettner, and I. Berbezier, Appl. Surf. Sci. **162**, 576 (2000).
[10] G. S. Higashi, Y. J. Chabal, G. W. Trucks, and K. Raghavachari, Appl. Phys. Lett. **56**, 656 (1990).
[11] H. Hibino, Y. Shinoda, Y. Kobayashi, and K. Sugii, Jpn. J. Appl.

Phys., Part 1 **30**, 1337 (1991).
[12] H. K. Shin, D. J. Lockwood, and J. M. Baribeau, Solid State Commun. **114**, 505 (2000).
[13] F. Boscherini, G. Capellini, L. Di Gaspare, F. Rosei, N. Motta, and S. Mobilio, Appl. Phys. Lett. **76**, 682 (2000).
[14] G. Renaud, R. Lazzari, C. Revenant, A. Barbier, M. Noblet, O. Ulrich, F. Leroy, J. Jupille, Y. Borensztein, C. R. Henry, J. P. Deville, F. Scheurer, J. Mane, and O. Fruchart, Science **300**, 1416 (2003).
[15] F. Poser, A. Bhattacharya, S. Weeke, and W. Richter, J. Cryst. Growth **248**, 317 (2003).
[16] T. Merdzhanova, S. Kiravittaya, A. Rastelli, M. Stoffel, U. Denker, and O. G. Schmidt, Phys. Rev. Lett. **96**, 226103 (2006).
[17] S. K. Sinha, E. B. Sirota, S. Garoff, and H. B. Stanley, Phys. Rev. B **38**, 2297 (1988).
[18] V. A. Shchukin, N. N. Ledentsov, and D. Bimberg, *Epitaxy of Nanostructures* (Springer-Verlag, Heidelberg, 2004).
[19] Y. D. Park, A. T. Hanbicki, S. C. Erwin, C. S. Hellberg, J. M. Sullivan, J. E. Mattson, T. F. Ambrose, A. Wilson, G. Spanos, and B. T. Jonker, Science **295**, 651 (2002).